

# On the Relation between $\pi$ Bonding, Electronegativity, and Bond Angles in High-Valent Transition Metal Complexes

Martin Kaupp\*<sup>[a]</sup>

**Abstract:** Ligand-to-metal  $\pi$  bonding is important for the understanding of bond angles in  $d^0$  transition metal complexes. This is demonstrated by density functional calculations on a number of model complexes, combined with natural bond orbital and natural localized molecular orbital analyses. Analyses of the simple model systems  $\text{ScF}_2^+$  and  $\text{ZrO}_2$  indicate a complicated dependence of  $\pi$  bonding on bond angle. In particular, in-plane  $\pi$  bonding exhibits a nonuniform dependence, whereas out-of-plane  $\pi$  bonding shows a more regular behavior. This may be understood from the nodal properties of the relevant metal  $d$  orbitals. The net  $\pi$  bonding behavior then depends sensitively on the donor properties of the ligands. While  $\pi$  bonding appears to favor the bent equilibrium structure for the “strong  $\pi$ -donor case”  $\text{ZrO}_2$ , it is more efficient

at a linear structure for the “weak  $\pi$ -donor case”  $\text{ScF}_2^+$ . Similar considerations come into play for more complicated species, exemplified by  $\text{MX}_2\text{Y}_2$  model complexes. Thus, the “inverse Bent’s rule structures” of  $\text{TiCl}_2(\text{CH}_3)_2$  and  $\text{TiCl}_2\text{H}_2$  are related to the improved in-plane  $\pi(\text{Ti}-\text{Cl})$  bonding at larger Cl-Ti-Cl angles. In contrast, for  $\text{CrO}_2\text{F}_2$  or  $\text{MoO}_2\text{F}_2$ , the angular dependences of the strong in-plane and out-of-plane components of  $\pi(\text{M}-\text{O})$  bonding compensate each other partially, and the O-M-O angles appear to be dominated by the  $\sigma$ -bonding framework. When

introducing a strong  $\sigma$ -bonding ancillary ligand, as in  $\text{CrO}_2\text{H}_2$ , the net  $\pi$  bonding does again seem to favor larger angles. Electronegativity effects on bond angles have been probed by studying heteroleptic complexes without significant  $\pi$  bonding. “Inverse structures” are found for complexes like  $\text{TiH}_2(\text{CF}_3)_2$  or  $\text{Ti}(\text{SiH}_3)_2(\text{CH}_3)_2$ , that is the smaller angles are those between the less electronegative ligands. Hybridization analyses indicate *less*  $d$  character for these bonds. The interpretation is complicated by the fact that even the structure for the silicon analogon of the latter complex violates Bent’s rule. In general, Bent’s rule appears to be less useful for  $d^0$  transition metal complexes than for main group compounds, in part due to the much larger importance of  $\pi$  bonding for the former.

**Keywords:** Bent’s rule • bond angles • density functional calculations • natural bond orbitals • natural localized molecular orbitals • transition metals

## I. Introduction

During the past decade an increasing number of early transition metal complexes in high oxidation states (mainly with  $d^0$  configurations, but also partly  $d^1$  and  $d^2$  systems) have been found to prefer structures that defy the valence shell electron pair repulsion (VSEPR) model or other simple structural rules derived for main group chemistry. Examples range from the famous bent dihalides of some heavy alkaline earth metals<sup>[1]</sup> to nonoctahedral structures of six-coordinate

organometallic complexes<sup>[2, 3, 4]</sup> like  $[\text{W}(\text{CH}_3)_6]$ ,  $[\text{Re}(\text{CH}_3)_6]$ , or  $[\text{Zr}(\text{CH}_3)_6]^{2-}$  (a more general overview on “non-VSEPR structures” for  $d^0$  complexes will be given elsewhere<sup>[5]</sup>). It has been demonstrated that the  $d$ -orbital participation in covalent  $\sigma$ -bonding contributions (enhanced by core polarization, at least for the earlier metals<sup>[6]</sup>) favors such distorted “non-VSEPR structures”. In addition to ligand repulsion,  $\pi$  bonding is usually considered to oppose the distortions, as it increases the gap between occupied and unoccupied MOs at the high-symmetry structures and thereby disfavors second-order orbital mixing upon symmetry lowering.<sup>[3, 7]</sup> Thus, for example, the Group 6 hexahalides are all octahedral, in contrast to their hexamethyl or hexahydride analogues. This is attributed largely to a better stabilization of the octahedron relative to the trigonal prism by  $\pi$  bonding.<sup>[3, 7a]</sup>

However, for some other systems,  $\pi$  bonding has been considered to favor small angles between multiply bonded ligands and thus strong deviations from the expectations of the VSEPR model. The most famous example is the *cis*

[a] Priv.-Doz. Dr. M. Kaupp  
Institut für Anorganische Chemie  
Universität Würzburg  
Am Hubland, D-97074 Würzburg (Germany)  
Fax: (+49) 931-888-4605  
E-mail: kaupp@mail.uni-wuerzburg.de.

Supporting information for this article (two figures with canonical MO energies for  $\text{ScF}_2^+$  and  $\text{ZrO}_2$ , one figure with NLMO analyses for  $\text{CrS}_2\text{F}_2$ , and one table with hybridization analyses) is available on the WWW under <http://www.wiley-vch.de/home/chemistry/> or from the author.

“molybdenyl fragment”,  $\text{MoO}_2^{2+}$ , which is present in many  $\text{Mo}^{\text{VI}}$  dioxo complexes<sup>[8, 9, 10]</sup> but has also recently been considered computationally as an isolated species.<sup>[11]</sup> Here  $\pi$  bonding is thought to contribute to the small O-Mo-O bond angles (around  $101-105^\circ$ ).<sup>[8, 11]</sup> Small O-M-O angles are also found for chromyl complexes,  $\text{CrO}_2\text{X}_2$ , and for a considerable number of related compounds. We will show here, by analyzing the results of density functional calculations, how these apparently contradictory views on the relation between  $\pi$  bonding and bond angles may be reconciled.

Another controversy has arisen over whether and how it is possible to extend Bent's rule to transition metal chemistry. An instructive example to start with is the distorted tetrahedral structure of  $\text{TiCl}_2(\text{CH}_3)_2$ . Gas-phase electron diffraction<sup>[12]</sup> and computation<sup>[13, 14]</sup> both indicate the C-Ti-C and Cl-Ti-C angles to be lower than the ideal tetrahedral value,

**Abstract in German:**  $\pi$ -Bindungsbeiträge zwischen Metall und Liganden spielen eine wichtige Rolle für das Verständnis von Bindungswinkeln in  $d^0$ -Übergangsmetallkomplexen. Dies zeigen Dichtefunktionalrechnungen an einer Reihe von Modellkomplexen, in Kombination mit natural bond orbital und natural localized molecular orbital Analysen. Die Untersuchung der einfachen Modellsysteme  $\text{ScF}_2^+$  und  $\text{ZrO}_2$  ergab einen komplizierten Zusammenhang zwischen  $\pi$ -Bindung und Bindungswinkel. Insbesondere weisen die in-plane  $\pi$ -Anteile eine nichtmonotone Abhängigkeit vom Winkel auf, während die out-of-plane  $\pi$ -Anteile sich regulär verhalten. Dies kann anhand des Knotenverhaltens der d-Orbitale am Metall verstanden werden. Der Winkelverlauf der Summe der  $\pi$ -Bindungsanteile hängt empfindlich von den  $\sigma$ - und  $\pi$ -Donoreigenschaften der Liganden ab. Während die  $\pi$ -Bindungen die gewinkelte Struktur des  $\text{ZrO}_2$  klar begünstigen, scheinen sie im  $\text{ScF}_2^+$  bei einer linearen Anordnung effizienter zu sein. Ähnliche Gesichtspunkte sind für kompliziertere  $\text{MX}_2\text{Y}_2$ -Systeme von Bedeutung. Tatsächlich scheint die „Inverse-Bent'sche-Regel-Struktur“ von  $\text{TiCl}_2(\text{CH}_3)_2$  und  $\text{TiCl}_2\text{H}_2$  mit verbesserter  $\pi(\text{Ti}-\text{Cl})$ -Bindung bei größeren Cl-Ti-Cl Winkeln zusammenzuhängen. Im Gegensatz dazu kompensieren sich die starken in-plane und out-of-plane  $\pi$ -Anteile für  $\text{CrO}_2\text{F}_2$  und  $\text{MoO}_2\text{F}_2$  teilweise, so daß anscheinend die  $\sigma$ -Bindungsanteile die O-M-O Winkel dominieren. Bei Einführung starker  $\sigma$ -Donoren als Nachbarliganden, wie im  $\text{CrO}_2\text{H}_2$ , scheinen die  $\pi$ -Anteile insgesamt wieder größere O-M-O Winkel zu begünstigen. Der Einfluß von Elektronegativitätseffekten wurde an heteroleptischen Komplexen ohne signifikante  $\pi$ -Bindung untersucht. „Inverse“ Strukturen wurden für Komplexe wie  $\text{TiH}_2(\text{CF}_3)_2$  oder  $\text{Ti}(\text{SiH}_3)_2(\text{CH}_3)_2$  gefunden, d. h. kleinere Winkel treten zwischen den weniger elektronegativen Liganden auf, wobei Hybridisierungsanalysen für diese Bindungen den geringeren d-Charakter am Metall ergeben. Die Interpretation wird dadurch kompliziert, daß selbst das Silizium-Analogon des letzten Komplexes die Bent'sche Regel verletzt. Allgemein scheint die Bent'sche Regel für  $d^0$ -Übergangsmetallkomplexe weniger nützlich zu sein als für Verbindungen der Hauptgruppenelemente, teilweise aufgrund der viel größeren Bedeutung der  $\pi$ -Bindungsbeiträge.

whereas the Cl-Ti-Cl angle is larger (Figure 1a). This is just opposite to what one normally observes in main group compounds, for example for the analogous  $\text{SiCl}_2(\text{CH}_3)_2$  compound (Figure 1b<sup>[15]</sup>). Here the angle between the less electronegative alkyl ligands is larger than tetrahedral, whereas the Cl-Si-Cl angle is smaller.

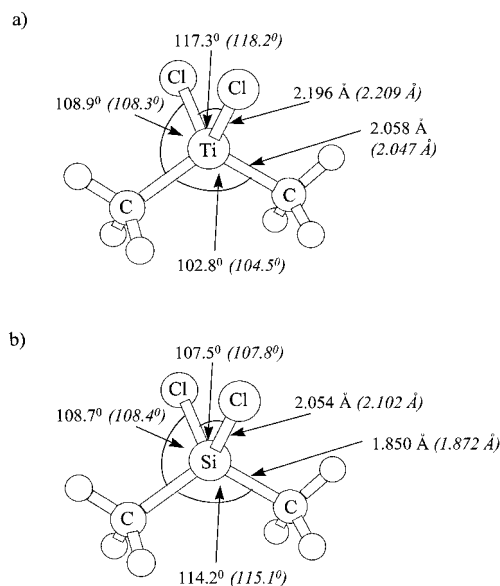


Figure 1. Main structural parameters for  $\text{MCl}_2(\text{CH}_3)_2$  complexes obtained from gas-phase electron diffraction, and from DFT calculations at the level used throughout this work (italic numbers in parentheses). a)  $\text{M}=\text{Ti}$  (experimental data from ref. [12]). b)  $\text{M}=\text{Si}$  (experimental data from ref. [15]).

The main group structures in such cases are frequently explained by Bent's rule,<sup>[16]</sup> which states that the bonds to the more electronegative substituents utilize more central-atom p-orbital character and thus make smaller angles, whereas the bonds to the less electronegative substituents obtain more s character and thus prefer larger angles (the valence p orbitals of main group atoms are higher in energy and have a larger radial extent than the valence s orbitals<sup>[17]</sup>). Jonas et al. argued,<sup>[14]</sup> on the basis of natural bond orbital (NBO) hybridization analyses for  $\text{TiCl}_2(\text{CH}_3)_2$  and related complexes, that Bent's rule has to be rephrased to be applicable to transition metal species. As the  $(n-1)d$  orbitals are lower in energy and have a smaller radial extent than the  $ns$  orbitals, the bonds to the less electronegative ligands tend to acquire more d character and thus make smaller angles, whereas the bonds to the more electronegative ligands have larger s character and thus make larger angles. This has been criticized by McGrady et al.<sup>[12]</sup> and by Landis et al.<sup>[18]</sup> In particular, Landis et al. argue that simple valence-bond hybrid-orbital strength functions calculated for the appropriate  $sd^x$  hybrids prefer larger bond angles with increasing  $x$ , that is with increasing d character. Thus, the less electronegative ligands should make the larger angles, just as predicted by Bent's rule. Landis et al. suggested that the “inverted” structures of  $\text{TiCl}_2(\text{CH}_3)_2$  and of related compounds may be explained instead within a valence-bond picture by invoking ionic resonance structures (this would imply lower d character in

the Ti–C compared to the Ti–Cl bonds).<sup>[18]</sup> We will show here that  $\pi$  bonding may be at least as important as electronegativity differences in controlling the bond angles in these and other systems, and that Bent's rule thus has only very limited applicability for most early transition metal complexes. Landis also pointed out<sup>[19]</sup> that the  $\sigma(\text{Ti}-\text{Cl})$  NBOs computed for  $\text{TiCl}_2(\text{CH}_3)_2$  indicate significant bond bending (i.e. the charge centroid of the NBO deviates from the straight line between the atoms), and we will address this point in our discussion.

## II. Computational methods

All calculations for the present paper have been carried out at the gradient-corrected density functional theory level, using the BP86 functional,<sup>[20]</sup> with the Gaussian94 program.<sup>[21]</sup> Quasirelativistic small-core effective-core potentials (ECPs) and (8s7p6d)/[6s5p3d] valence basis sets were used for the transition metals,<sup>[22]</sup> together with ECPs<sup>[23]</sup> and (4s4p1d)/[2s2p1d] valence basis sets<sup>[1c, 23, 24]</sup> for the p-block main group atoms. Hydrogen basis sets were of the size (4s)/[2s],<sup>[25]</sup> augmented by one p-function ( $\alpha = 1.0$ ) for hydrogen atoms directly bonded to the metal. To get information on energies and bonding as a function of bond angles, the angles in question have been varied stepwise, and all other degrees of freedom have been reoptimized at each angle value.

Natural population analyses (NPA), natural bond orbital (NBO), and natural localized molecular orbital (NLMO) analyses<sup>[26, 27]</sup> have been carried out with the built-in NBO subroutines of the Gaussian94 program.<sup>[21]</sup> Desired Lewis structures based on a representation of the one-particle density matrix in the basis of strictly localized NBOs have been selected by the \$CHOOSE keyword of the NBO code if necessary. The composition and hybridization of natural atomic orbital (NAO) contributions to the NLMOs derived from this NBO Lewis structure have been used as the main quantities in the present analyses. We consider the composition and hybridization analysis of the NLMOs to be more appropriate here than either the analysis of the strictly localized NBOs used by Jonas et al.,<sup>[14]</sup> or the Mulliken analysis of Boys localized orbitals used by McGrady et al.<sup>[12]</sup> (or much earlier in a related context by Kutzelnigg<sup>[17]</sup>). While the former method is not recommended due to the large part of the one-particle density matrix that has to be typically assigned to “antibonding” or “Rydberg-type” NBOs for transition metal complexes, the latter scheme suffers from the large basis-set dependency and from other known artefacts of the Mulliken population analysis. We found triply bonded  $|\text{X}\equiv\text{M}\equiv\text{X}|$  Lewis structures to be most appropriate for  $\text{ScF}_2^+$  and  $\text{ZrO}_2$  (see Section III), and for the  $\text{MX}_2$  fragments of the dichalcogenido complexes (see Section IV.B). For the  $\text{MCl}_2\text{Y}_2$  ( $\text{M} = \text{Si}, \text{Ti}; \text{Y} = \text{H}, \text{CH}_3$ ) complexes (see Section IV.A), NBO Lewis structures with only single bonds were better behaved (they accounted for a larger fraction of the electronic charge density), and the metal contributions to the corresponding  $\pi$ -type chlorine lone-pair NLMOs were analyzed. Singly bonded Lewis structures were

of course used for exclusively  $\sigma$ -bonded systems (Section IV.C).

NBO deletion analyses<sup>[26b, 27]</sup> have been based on singly bonded NBO Lewis structures. Those off-diagonal NBO Fock-matrix elements were deleted which couple the  $\pi$ -type lone-pair NBOs on the ligand atom in question (Cl for  $\text{MCl}_2\text{Y}_2$  complexes) to “antibonding” and “Rydberg-type” NBOs. We considered contributions from individual matrix elements on the order of maximally about 40–60  $\text{kJ mol}^{-1}$  to the second-order perturbation theoretical analysis of the NBO Fock-matrix to indicate a good NBO Lewis structure. No deletion analyses were carried out for cases where significantly larger interactions were found. The energy of the truncated NBO Fock-matrix was computed by performing one extra SCF iteration, to obtain the “energy for an NBO Lewis structure” ( $E_{\text{Lewis}}$ ).<sup>[26b, 27]</sup> As no analytical energy gradients are available for this non-self-consistent energy, the corresponding structure optimizations have been carried out numerically. We note in passing that the Kohn–Sham wavefunctions used here refer to a hypothetical noninteracting reference system. However, it has been shown that they form a well-suited starting point for the analysis of the electronic structure of the real system as well.<sup>[28]</sup>

## III. The triatomic case: $\pi$ bonding in $\text{ScF}_2^+$ versus $\text{ZrO}_2$

The simplest case that may be considered is that of a triatomic  $d^0 \text{MX}_2$  system. It appears reasonable to assume, based on many calculations for such early transition metal compounds, that the metal d orbitals dominate the bonding, with the s-orbital contributions being somewhat less important, and the p-orbital contributions being small (see, e.g., refs. [2a, 18], but also ref. [29]). Those metal d orbitals that may form  $\sigma$  bonds with the appropriate ligand orbital combinations are indicated in Figure 2a for the linear and in Figure 2b for the bent structure (the symmetry labels and coordinate axes generally refer to  $C_{2v}$  symmetry). The unsymmetrical combination of the ligand  $\sigma$ -type orbitals ( $b_2$  symmetry) finds an

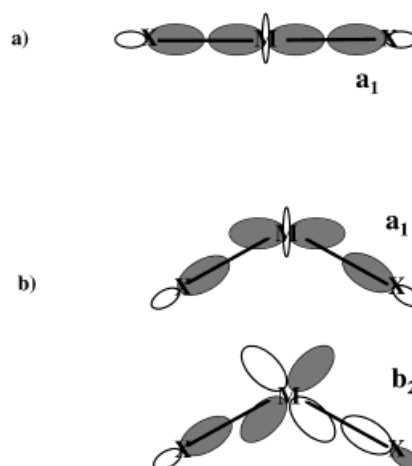


Figure 2. Metal d orbitals available as  $\sigma$ -bonding acceptors for a) linear, and b) bent  $\text{MX}_2$  complexes. See also ref. [30].

appropriate d orbital ( $d_{yz}$ ) only at a bent structure (it may only interact with a metal  $p_y$  orbital at the linear structure). This is generally accepted to be a major driving force for the bending of such  $d^0$   $\text{MX}_2$  systems.<sup>[1, 7, 30]</sup> The simultaneous loss of overlap of the symmetrical combination with the  $d_{x^2-y^2}$  ( $a_1$ ) orbital is considered to be of lesser importance.

Those metal d orbitals available to accept charge density from ligand  $\pi$ -type lone pairs are shown in Figure 3. For the linear structure (Figure 3a), the four possible linear combinations of ligand  $\pi$ -type lone pairs find only two d orbitals to interact with ( $d_{xy}$  and  $d_{yz}$ —in  $C_{2v}$  symmetry these orbitals belong to  $a_2$  and  $b_2$ , respectively). The three metal d orbitals that may in principle contribute to  $\pi$  bonding at the bent structure (Figure 3b) are  $d_{xy}$  ( $a_2$ ),  $d_{xz}$  ( $b_1$ ), and  $d_{z^2}$  ( $a_1$  symmetry, metal s and  $d_{x^2-y^2}$  AO contributions may be mixed in). The former two orbitals may be considered to be out-of-plane  $\pi$  bonding ( $\pi_{op}$ ), whereas the latter may be termed in-plane  $\pi$  bonding ( $\pi_{ip}$ ).

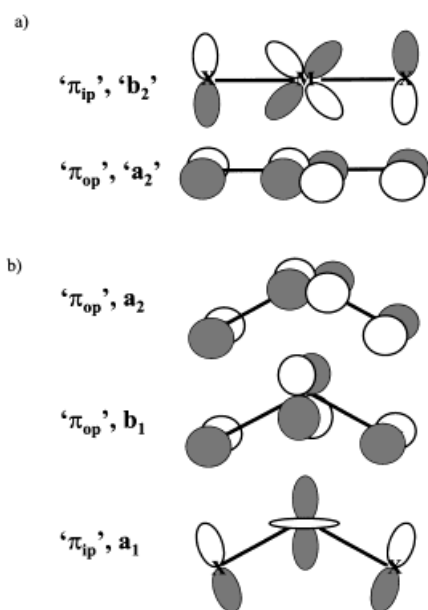


Figure 3. Metal d orbitals available as  $\pi$ -bonding acceptors for a) linear, and b) bent  $\text{MX}_2$  complexes. See also refs. [8b,11].

This is not new. These orbitals and their influence on bonding have been discussed by various workers.<sup>[8, 11]</sup> However, let us consider in somewhat more detail which changes in  $\pi$  bonding may be expected to happen upon bending such an  $\text{MX}_2$  molecule. Starting from the linear structure (bending angle  $\alpha = 180^\circ$ ), we first lose any in-plane  $\pi$  bonding from the  $d_{yz}$  ( $b_2$ ) orbital, as the overlap with the ligand orbitals decreases rapidly (at the same time this  $d_{yz}$  orbital starts to be involved more efficiently in  $\sigma$  bonding, cf. Figure 1b). Loss of  $\pi_{op}$  overlap by the  $d_{xy}$  ( $a_2$ ) orbital is expected to be much less pronounced. As we lower the angle further, the  $d_{xz}$  ( $b_1$ ) orbital becomes slowly  $\pi_{op}$  bonding, and then the  $a_1$  orbital (composed of  $d_{z^2}$ ,  $d_{x^2-y^2}$ , and s character) becomes more suddenly  $\pi_{ip}$  bonding. To a first approximation, we expect thus only moderate, uniform changes in  $\pi_{op}$  bonding with decreasing angle, as the slow loss of overlap with the  $d_{xy}$  ( $a_2$ ) orbital should be roughly compensated by better overlap with the  $d_{xz}$

( $b_1$ ) orbital. On the other hand, we expect a notable loss of  $\pi_{ip}$  bonding upon bending at larger angles, before the  $d_{z^2}$  ( $a_1$ ) orbital may start to contribute at smaller angles, and  $\pi_{ip}$  bonding starts to increase again.

These simple considerations suggest that the overall  $\pi$  bonding will not be a uniform function of bond angle (in particular due to the behavior of  $\pi_{ip}$  bonding). Owing to competition between  $\pi_{ip}$  and  $\sigma$  bonding, we may expect that the change of  $\pi$  bonding with bond angle will also depend on the relative  $\sigma$ - and  $\pi$ -donor abilities of the ligands. Let us compare the  $\text{ScF}_2^+$  ion as an example with weak  $\pi$ -donor ligands and the gas-phase molecule  $\text{ZrO}_2$  as an example with strong  $\pi$ -donor ligands. Both systems have previously been studied computationally<sup>[31, 32]</sup> ( $\text{ZrO}_2$  also experimentally<sup>[31b]</sup>) and were found to be significantly bent. Table 1 summarizes

Table 1. DFT-optimized structures for  $\text{ScF}_2^+$  and  $\text{ZrO}_2$ .

	$\angle(\text{X-M-X}) [^\circ]$	$d(\text{M-X}) [\text{\AA}]$	$\Delta E [\text{kJ mol}^{-1}]^{\text{[a]}}$
$\text{ScF}_2^+$	112.2	1.772	64.5
	(180) <sup>[b]</sup>	1.808	
$\text{ZrO}_2$	106.1	1.796	246.0
	(180) <sup>[b]</sup>	1.876	

[a] Linearization energy. [b] Optimization restricted to linear structure.

our DFT-optimized structural data, together with the bond lengths at enforced linear structures, and with the linearization energies. Our results agree well with previous ab initio studies.<sup>[31, 32]</sup> The somewhat more covalent  $\text{ZrO}_2$  compound has a smaller angle, a considerably larger linearization energy, and it shows a more pronounced bond contraction upon bending (0.080  $\text{\AA}$  vs. 0.036  $\text{\AA}$ ) than the more ionic  $\text{ScF}_2^+$  ion (we have chosen  $\text{ZrO}_2$  rather than the 3d-analogue  $\text{TiO}_2$ , to ensure an overall similar bond polarity in both complexes<sup>[33]</sup>). Figure 4 illustrates the much steeper bending potential of the zirconium compound.

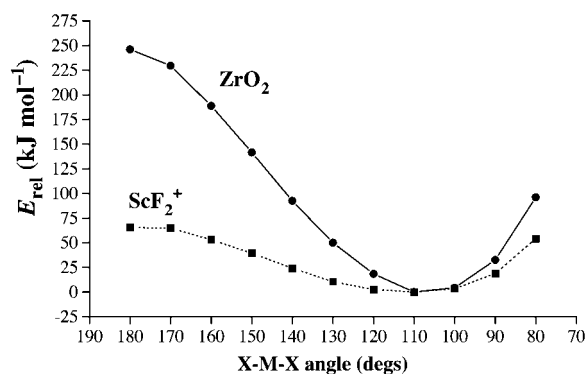


Figure 4. Comparison of calculated bending potential curves for  $\text{ScF}_2^+$  and  $\text{ZrO}_2$ .

The origin of the differences between the two systems may be traced in different ways, for example based on canonical (delocalized) or on localized orbitals. Throughout this work we will emphasize a localized orbital viewpoint. As may be seen from Figures 1 and 2, at a bent structure in-plane  $\pi$  and  $\sigma$  bonding is not well defined from a symmetry point of view (in

contrast,  $\pi_{\text{op}}$  bonding may be identified clearly). At the canonical MO level it is particularly difficult to separate  $\pi_{\text{ip}}$  and  $\sigma$  bonding contributions, as these tend to employ the same MOs (of  $b_2$  and  $a_1$  symmetries), to an extent that changes dramatically with the bond angle. This orbital mixing is most pronounced for the more covalent  $\text{ZrO}_2$  and complicates the analysis. Some of the differences between  $\text{ScF}_2^+$  and  $\text{ZrO}_2$  are nevertheless apparent already at the canonical MO level (see Figures S1 and S2 in Supporting Information for the MO energies as a function of bond angle) and deserve mention. At the equilibrium structure, the symmetrical  $\pi_{\text{ip}}$  bonding  $a_1$  MO is relatively high in energy (above both  $\sigma$  bonding MOs) and has little metal character for  $\text{ScF}_2^+$ . In contrast, for  $\text{ZrO}_2$  the same MO is the lowest of the overall five MOs depicted in Figures 2b and 3b and has considerable metal character. Significant  $\pi_{\text{op}}$  bonding from both the  $a_2$  and  $b_1$  MOs (Figure 3b) is apparent for both systems, but again more pronouncedly so for  $\text{ZrO}_2$ .

Mixing between  $\sigma$  and  $\pi_{\text{ip}}$  bonding is also present in a localized MO picture and manifests itself in a deviation of the charge centroids of the localized  $\sigma$  bonding MOs from the internuclear axis (we will discuss the NLMOs but find similar effects also with other localization schemes), as well as a concomitant rotation of the  $\pi_{\text{ip}}$  bonding LMOs within the  $\text{MX}_2$  plane. For the two  $\text{MX}_2$  complexes, this “bond bending” is most pronounced at angles between  $150^\circ$  and  $170^\circ$  and below  $90^\circ$ , where the ligand hybrids deviate from the bond axis by  $30\text{--}45^\circ$  (the metal hybrids generally deviate less from the internuclear axis, typically only by a few degrees). It is thus clear that a designation as  $\sigma$  and  $\pi_{\text{ip}}$  bonding localized orbitals is not very well defined at these angles. Near the equilibrium bond angles this bond bending is less pronounced (generally below  $20^\circ$ ), and no such complications arise at  $180^\circ$ . Therefore, an analysis in terms of NLMO compositions appears to provide us with a somewhat more transparent interpretation than the canonical MOs, in spite of this inherent ‘bond bending’. We note that the  $\sigma/\pi_{\text{ip}}$  mixing is much more pronounced for the  $d^0$  complexes than for comparable main group species and appears to be a characteristic feature of the involvement of metal d orbitals. At small bond angles, the  $\pi_{\text{ip}}$  bonding ligand hybrids are rotated towards the second ligand, whereas at large angles they are rotated away. Closer inspection of the NLMOs indicates that this is related to improved involvement of the metal  $d_{z^2}$  AO in the symmetrical in-plane  $\pi$ -MO ( $a_1$ , cf. Figure 2b) at smaller angles but improved involvement of the metal  $d_{x^2-y^2}$  AO at large angles. The  $\sigma$  bonding NBOs and NLMOs deviate from the bond axis just in the opposite direction than the  $\pi_{\text{ip}}$  bonding NLMOs (most likely due to competition for the  $d_{z^2}$  and  $d_{x^2-y^2}$  AOs).

We will analyze in the following the relative metal contributions (in %) to the natural localized MOs (NLMOs), corresponding to  $\sigma$ ,  $\pi_{\text{ip}}$ , and  $\pi_{\text{op}}$  bonding between M and X, as a function of bond angle. These values are a useful measure of the covalency of  $\sigma$ ,  $\pi_{\text{ip}}$ , and  $\pi_{\text{op}}$  bonding, and we may associate with them also, to a first approximation, the relative strengths of these covalent interactions (keeping in mind the inherent limitations in the definition of the  $\sigma$  and  $\pi_{\text{ip}}$  components). Results for  $\text{ScF}_2^+$  and  $\text{ZrO}_2$  are given in Figures 5 and 6, respectively.

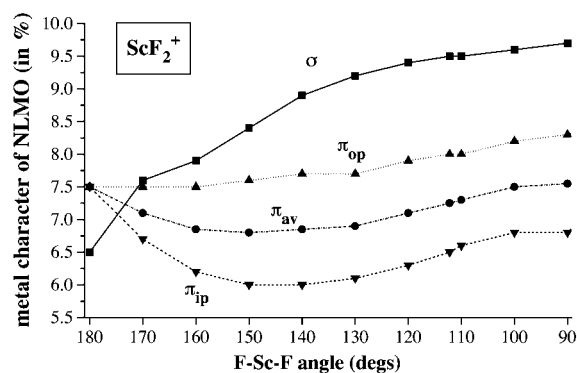


Figure 5. Dependence of the metal character (in%) of the bonding NLMOs in  $\text{ScF}_2^+$  on X-M-X angle (starting from a  $|\text{X}=\text{M}=\text{X}|$  Lewis structure).

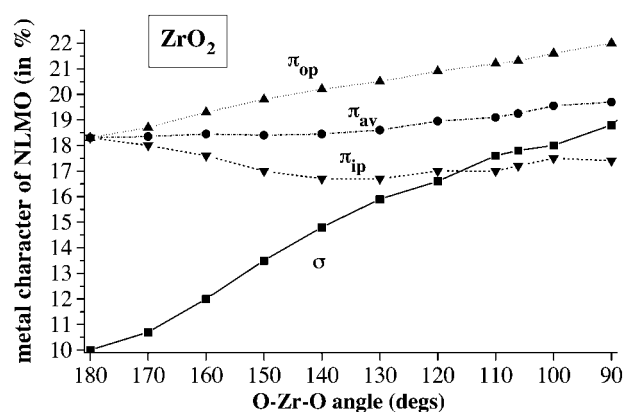


Figure 6. Dependence of the metal character (in%) of the bonding NLMOs in  $\text{ZrO}_2$  on X-M-X angle.

Before discussing the angular dependence of the NLMO composition, we note that the more covalent character of the bonding in  $\text{ZrO}_2$  compared to  $\text{ScF}_2^+$  is shown nicely by the larger metal character of both  $\sigma$ - and  $\pi$ -type NLMOs (consequently, the overall changes of these values as a function of bond angle are also larger). However, the  $\sigma$  covalency is significantly larger than either  $\pi_{\text{ip}}$  or  $\pi_{\text{op}}$  covalency for  $\text{ScF}_2^+$ , except for the largest angles. In contrast, for  $\text{ZrO}_2$  the  $\sigma$  covalency becomes comparable to the  $\pi_{\text{ip}}$  covalency only around the equilibrium bond angles, and  $\pi_{\text{op}}$  covalency is larger at all angles. This is consistent with our designation of  $\text{ScF}_2^+$  as a complex with weak  $\pi$ -donor ligands, and of  $\text{ZrO}_2$  as a complex with strong  $\pi$  bonding. The  $\pi_{\text{ip}}$  curve remains generally below the  $\pi_{\text{op}}$  curve in both complexes, except of course at  $180^\circ$ , where the two curves meet. This confirms that in-plane  $\pi$  bonding is generally weaker than out-of-plane  $\pi$  bonding for bent  $\text{MX}_2$   $d^0$  systems, consistent with the rotational barriers and conformational preferences computed previously for complexes like  $\text{Ba}(\text{NH}_2)_2$ .<sup>[34]</sup> As expected,  $\sigma$  bonding does in both cases become dramatically more covalent as the angle decreases. The uniform increase in  $\sigma$  covalency continues down to about  $90^\circ$ .

Let us now turn to the angular dependence of  $\pi$  bonding. In agreement with our above considerations, an essentially uniform increase of  $\pi_{\text{op}}$  covalency from  $\alpha=180^\circ$  down to  $\alpha=90^\circ$  is apparent. This increase is much more pronounced for  $\text{ZrO}_2$  (from 18.3% to 22.0% relative metal character) than

for  $\text{ScF}_2^+$  (from 7.5 % to 8.3 %). The behavior of  $\pi_{\text{ip}}$  covalency is quite different and also appears to follow the above discussion: A decrease upon bending is found at large angles, before the curve rises again at lower angles. In both systems, the minimum of the  $\pi_{\text{ip}}$  curve is found near  $150^\circ$  angles. The minimum value is about 6.0 % for  $\text{ScF}_2^+$  and about 13.5 % for  $\text{ZrO}_2$ . This is about 1.5 % and about 4.8 %, respectively, below the corresponding value at  $\alpha = 180^\circ$ . At the corresponding equilibrium bond angles, the metal contribution to the  $\pi_{\text{ip}}$  NLMO is in both cases still about 1 % below the value at  $\alpha = 180^\circ$ .

However, let us consider the overall  $\pi$  bonding, that is the average ( $\pi_{\text{av}}$ ) of both  $\pi_{\text{ip}}$  and  $\pi_{\text{op}}$  covalency: For  $\text{ScF}_2^+$ , the  $\pi_{\text{av}}$  curve does have a notable minimum around  $\alpha = 150^\circ$ , and the value at the equilibrium bond angle (7.25 % at  $112.2^\circ$ ) is slightly lower than at  $180^\circ$ . In contrast, due to the notable increase in  $\pi_{\text{op}}$  covalency with decreasing angle, the  $\pi_{\text{av}}$  curve for  $\text{ZrO}_2$  has only a very slight dip around  $150^\circ$ , and the  $\pi_{\text{av}}$  value at the equilibrium bond angle (ca. 19.25 % at  $106.1^\circ$ ) is larger than at  $180^\circ$ . We expect therefore that  $\pi$  bonding *increases* the energy difference between bent equilibrium structure and linear arrangement for  $\text{ZrO}_2$ , whereas it should *decrease* the energy gain upon bending for  $\text{ScF}_2^+$ . However, in both systems, the  $\pi_{\text{av}}$  curve has a positive slope around the equilibrium bond angle (this is much more pronounced for  $\text{ZrO}_2$ ). Thus, the actual bond angle should be reduced by  $\pi$  bonding. Attempts to confirm this conclusion by NBO deletion analyses have failed, as singly bonded NBO Lewis structures did not describe the one-particle density matrix well for these systems. Thus, in contrast to the more favorable situation for the  $\text{MCl}_2\text{Y}_2$  systems discussed in the following section, we cannot provide additional support for the NLMO results by a complete NBO deletion analysis (but the deletion energies obtained do at least seem to suggest that  $\pi$  bonding favors indeed the linear structure).

In a recent DFT study of the metallocenes  $[\text{M}(\eta^5\text{-C}_5\text{H}_5)_2]$  ( $\text{M} = \text{Ca}, \text{Sr}$ ),<sup>[35]</sup> the symmetrical  $\pi_{\text{ip}}$  bonding combination ( $a_1$  in Figure 2b) has been held responsible as the main origin of bent structures. Unfortunately, the significantly bent metallocene structures in that work appear to be artefacts of the unbalanced basis sets used<sup>[36]</sup> and contrast with earlier MP2 results<sup>[37]</sup> which give quasilinear structures (i.e. very shallow bending potentials). However, one may indeed speculate about the interesting question of significant  $\pi_{\text{ip}}$ -bonding contributions in more strongly bent metallocene structures, such as those found computationally for the  $[\text{M}(\eta^5\text{-C}_5\text{H}_5)_2]^+$  ( $\text{M} = \text{Sc}, \text{La}$ ) ions,<sup>[38]</sup> or experimentally in bent metallocene complexes with additional ligands. Of course, the discrimination between  $\sigma$  and  $\pi_{\text{ip}}$  bonding will be even less straightforward in these cases than for the present model systems.

#### IV. Is Bent's rule applicable to transition metal systems?

##### A. Comparison of $\text{MCl}_2\text{Y}_2$ ( $\text{M} = \text{Ti}, \text{Si}; \text{Y} = \text{H}, \text{CH}_3$ )

Let us now analyze the "inverse Bent's rule structure" of  $\text{TiCl}_2(\text{CH}_3)_2$  compared to the conventional structure of its

main group analogon  $\text{SiCl}_2(\text{CH}_3)_2$  (Figure 1). Figure 7 analyzes the covalency of the different metal-ligand  $\sigma$ - and  $\pi$  bonding NLMOs for  $\text{SiCl}_2(\text{CH}_3)_2$ . Figure 8 gives the results for  $\text{TiCl}_2(\text{CH}_3)_2$ , Figure 9 those for the simpler model complex  $\text{TiCl}_2\text{H}_2$ , for which we will discuss an NBO deletion analysis further below. The NLMO plot for  $\text{SiCl}_2\text{H}_2$  is very similar to that shown for the methyl compound, except for the less polar Si-H bond, and is omitted.

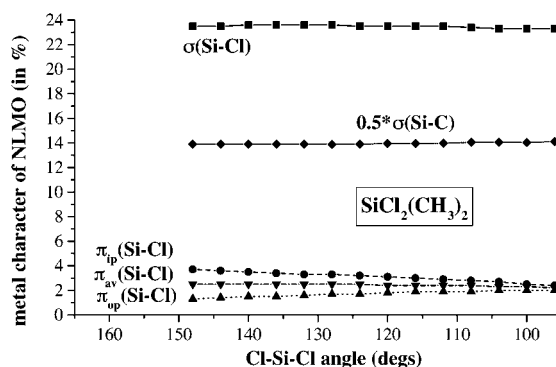


Figure 7. Dependence of the metal character (in %) of the bonding NLMOs in  $\text{SiCl}_2(\text{CH}_3)_2$  on Cl-M-Cl angle.

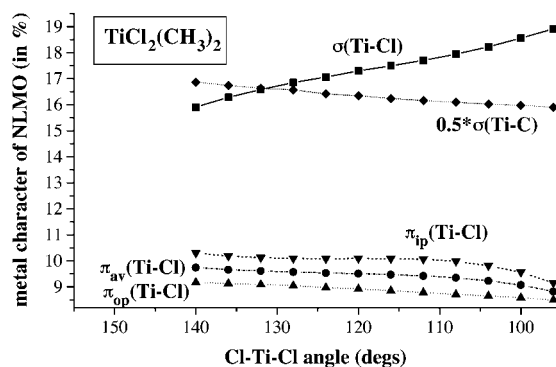


Figure 8. Dependence of the metal character (in %) of the bonding NLMOs in  $\text{TiCl}_2(\text{CH}_3)_2$  on Cl-M-Cl angle.

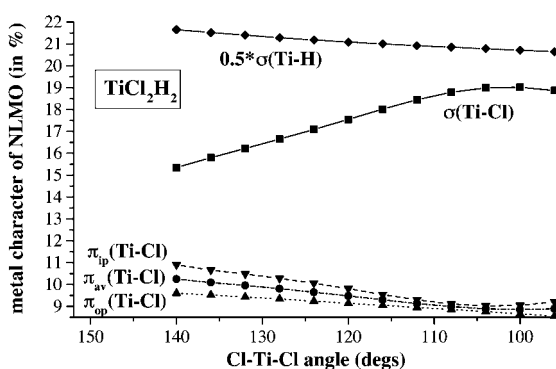


Figure 9. Dependence of the metal character (in %) of the bonding NLMOs in  $\text{TiCl}_2\text{H}_2$  on Cl-M-Cl angle.

First of all, we note that the M-Cl  $\pi$ -bonding covalency of the silicon complex is very low, with average metal contributions around 2 % compared to about 23–24 % for the Si-Cl  $\sigma$  bonding NLMO and about 28 % for the  $\sigma(\text{Si-C})$  NLMO (the latter curve was scaled by 0.5 in Figure 7 for a better

representation). This is not surprising, as the main group element silicon has only *outer* 3d orbitals available as  $\pi$  acceptors, and therefore most of the  $\pi$  bonding is only possible due to negative hyperconjugation at the expense of Si–C and Si–Cl  $\sigma$  bonding strength.<sup>[39]</sup> Changes of all curves along the Cl–Si–Cl angle coordinate are smooth and not very pronounced. The decrease of the  $\pi_{ip}$  curve with decreasing angle is almost compensated by the increasing  $\pi_{op}$  curve, such that the overall  $\pi$ -bonding covalency ( $\pi_{av}$ ) changes very little. We expect therefore that the influence of  $\pi$  bonding on the bond angles is moderate (as a result of the low  $\pi$  bonding, bond bending of the Si–Cl bonding NLMOs is small, typically below 5° in the relevant angle range).

The M–Cl  $\pi$ -bonding covalency for the Ti complexes (Figures 8 and 9) is considerably larger than for the silicon analogues, with about 9–10% metal contribution on average for both systems. Thus,  $\pi$  bonding is much more important for the  $d^0$  systems, due to the ready availability of *inner* 3d orbitals as  $\pi$  acceptors (this is also reflected in the much smaller difference between M–Cl and M–C distances than in the silicon analogue, cf. Figure 1). Nevertheless, with regard to the  $\sigma$  covalency, the chloride ligand may be classified as a weak  $\pi$  donor compared to the situation for ZrO<sub>2</sub> above.

Another notable feature in both complexes is the significant deviation of the chlorine hybrid contributions to the  $\sigma(\text{Ti–Cl})$  and  $\pi_{ip}(\text{Ti–Cl})$  NBOs and NLMOs from the bond axes (bond bending is again much less pronounced on the metal hybrid side, generally below ca. 5°). The chlorine  $\pi_{ip}$  hybrids bend towards the second chlorine ligand only at very small angles (below ca. 92° for TiCl<sub>2</sub>(CH<sub>3</sub>)<sub>2</sub>, below ca. 104° for TiCl<sub>2</sub>H<sub>2</sub>; around the angles mentioned, the magnitude of the bond bending exhibits a minimum) and point increasingly away from the second chlorine atom with larger Cl–Ti–Cl angles. As in the case of the MX<sub>2</sub> complexes (Section III), the opposite behavior is found for the  $\sigma$ -bonding hybrids. In the relevant angles range from about 105–125°, this rotation of the hybrids away from the bond directions is around about 20–30°. This has to be kept in mind when discussing the  $\pi_{ip}$  and  $\sigma$  covalency. Consequences of this bond bending for the metal hybridization will be discussed in Section IV C.

Interestingly, the  $\pi_{ip}$  covalency is slightly larger than the  $\pi_{op}$  covalency for both Ti complexes, as well as for the Si systems. The  $\pi_{op}$  covalency, and particularly the  $\pi_{ip}$  covalency, decrease with decreasing angles for both complexes ( $\pi_{ip}$  covalency starts to increase again slightly below 105° for TiCl<sub>2</sub>H<sub>2</sub>, see Figure 9). Over the angle range of interest (i.e. between 125° and 105°), the  $\pi_{av}$  curve has thus a negative slope in both systems. This negative slope is most pronounced for TiCl<sub>2</sub>H<sub>2</sub> (possibly due to the larger  $\sigma(\text{Ti–H})$  covalency, and to a somewhat lower  $\sigma(\text{Ti–Cl})$  covalency in this system). Thus, Ti–Cl  $\pi$  bonding may be considered to *increase* the Cl–Ti–Cl angle for both TiCl<sub>2</sub>(CH<sub>3</sub>)<sub>2</sub> and TiCl<sub>2</sub>H<sub>2</sub>.

To obtain further support for these findings, we have carried out NBO deletion analyses on TiCl<sub>2</sub>H<sub>2</sub> and SiCl<sub>2</sub>H<sub>2</sub>. The nondiagonal NBO Fock matrix elements involving the chlorine  $\pi$ -type lone pair NBOs were deleted. The structures optimized with respect to the energy of this singly bonded NBO Lewis structure ( $E_{\text{Lewis}}$ ) are compared in Table 2 to the fully optimized structures (cf.  $E_{\text{opt}}$ ). The energy loss upon

Table 2. NBO deletion analysis of  $\pi$ -bonding influences on the structures of MCl<sub>2</sub>H<sub>2</sub> (M = Ti, Si).

	$d(\text{M–Cl})$ [Å]	$d(\text{M–H})$ [Å]	$\angle(\text{Cl–M–Cl})$ [°]	$\angle(\text{H–M–H})$ [°]	$\angle(\text{Cl–M–H})$ [°]
TiCl <sub>2</sub> H <sub>2</sub>					
$E_{\text{opt}}^{\text{[a]}}$	2.177	1.685	119.9	109.3	106.8
$E_{\text{Lewis}}^{\text{[b]}}$	2.581	1.806	95.4	122.4	108.9
SiCl <sub>2</sub> H <sub>2</sub>					
$E_{\text{opt}}^{\text{[a]}}$	2.080	1.489	110.5	113.1	108.3
$E_{\text{Lewis}}^{\text{[b]}}$	2.232	1.488	97.1	120.3	109.2

[a] Fully optimized structure parameters. [b] Structure parameters optimized with truncated NBO Fock matrix, based on M–Cl and M–H single bonds only (i.e. M–Cl  $\pi$  bonding is “removed”). See Computational Methods.

deletion of the  $\pi$ -bonding contributions is considerably larger for M = Ti than for M = Si (689 kJ mol<sup>−1</sup> versus 266 kJ mol<sup>−1</sup> at the  $E_{\text{opt}}$  structures). These absolute energy values should not be overinterpreted, but their relative magnitude confirms the much larger importance of  $\pi$  bonding for the transition metal complex. In both MCl<sub>2</sub>H<sub>2</sub> systems, the  $E_{\text{Lewis}}$  structure conforms to Bent’s rule, that is the H–M–H angles are considerably larger than the tetrahedral value, whereas the Cl–M–Cl angles are smaller. In both cases,  $\pi$  bonding appears to counteract these electronegativity preferences. This has been found previously for other main group compounds.<sup>[39]</sup> The fully optimized structure of SiCl<sub>2</sub>H<sub>2</sub> still adheres to Bent’s rule, albeit with reduced deviations from ideal tetrahedral angles (and with the Cl–Si–Cl angle slightly above 109.5°). In contrast, the influence of  $\pi$  bonding for TiCl<sub>2</sub>H<sub>2</sub> is so large that it apparently reverses the structural preference in favor of large Cl–Ti–Cl, and low H–Ti–H and H–Ti–Cl angles.<sup>[40]</sup> We expect similar behavior for TiCl<sub>2</sub>(CH<sub>3</sub>)<sub>2</sub> (see Figure 8).

The ‘bending’ of the  $\pi_{ip}$  NBOs might lead us to overestimate the structural effect of  $\pi$  bonding. Nevertheless, the NBO Fock-matrix deletion analyses seem to support our suggestion that the apparent inversion of Bent’s rule for the TiCl<sub>2</sub>Y<sub>2</sub>  $d^0$  systems is at least in part due to the much larger M–Cl  $\pi$ -bonding contributions compared to those for the main group case. Whether larger angles may thus be expected in general between moderate  $\pi$  donors like halogen in the presence of strong ancillary  $\sigma$  donors, will have to be confirmed by further calculations (see also below).

## B. Chromyl fluoride and related complexes

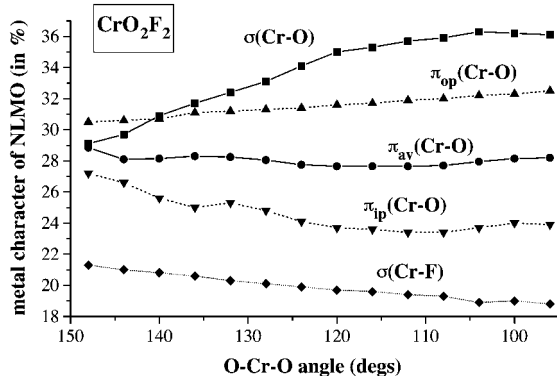
$\pi$  Bonding was rejected as a likely explanation for the “inverted” structure of TiCl<sub>2</sub>(CH<sub>3</sub>)<sub>2</sub> by McGrady et al.<sup>[12]</sup> They pointed out that the O–M–F and O–M–O bond angles in CrO<sub>2</sub>F<sub>2</sub> and VOF<sub>3</sub> are smaller than tetrahedral, in spite of the presumably larger  $\pi$ -bonding ability of oxo versus fluoro ligands. This is a valid argument. However, as shown above for the simpler systems ScF<sub>2</sub><sup>+</sup> and ZrO<sub>2</sub>, the angular dependence of  $\pi$  bonding for good  $\pi$  donors such as oxo ligands may differ significantly from the weak  $\pi$ -donor case. We also have to keep in mind the donor properties of the ancillary ligands (cf. above). Let us thus examine CrO<sub>2</sub>F<sub>2</sub> and related complexes. The optimized structures of a number of  $d^0$  dichalcogenido complexes are summarized in Table 3. We have included further CrO<sub>2</sub>Y<sub>2</sub> complexes (Y = Cl, H, CH<sub>3</sub>), as well as two

Table 3. DFT-optimized structures for chromyl fluoride and some related complexes.

$\text{MX}_2\text{Y}_2$	$d(\text{M}-\text{X})$ [Å]	$d(\text{M}-\text{Y})$ [Å]	$\angle(\text{X}-\text{M}-\text{X})$ [°]	$\angle(\text{Y}-\text{M}-\text{Y})$ [°]	$\angle(\text{X}-\text{M}-\text{Y})$ [°]
$\text{CrO}_2\text{F}_2$	1.571	1.715	108.5	110.6	109.4
$\text{CrO}_2\text{Cl}_2$	1.573	2.131	109.2	110.9	109.2
$\text{CrO}_2\text{H}_2$	1.566	1.578	112.0	126.2	104.7
$\text{CrO}_2(\text{CH}_3)_2$	1.578	1.972	112.6	114.0	107.6
$\text{MoO}_2\text{F}_2$	1.710	1.870	106.3	113.2	109.4
$\text{MoO}_2\text{Cl}_2$	1.710	2.275	106.5	112.6	109.3
$\text{WO}_2\text{F}_2$	1.728	1.878	106.3	115.7	108.6
$\text{WO}_2\text{Cl}_2$	1.729	2.285	106.3	114.2	109.0
$\text{CrS}_2\text{F}_2$	2.002	1.721	109.1	112.2	108.9
$\text{SO}_2\text{F}_2$	1.443	1.607	126.1	94.4	107.9
$\text{SO}_2\text{H}_2$	1.467	1.396	124.5	97.1	107.9

molybdenyl and two tungstyl dihalides, and the dithio analogue of chromyl fluoride,  $\text{CrS}_2\text{F}_2$ . The optimized structural parameters are in good agreement with experiment<sup>[41]</sup> and with other quantum chemical calculations,<sup>[42]</sup> where available. In general, the Y-M-Y angle is larger than the ideal tetrahedral value, only slightly so for  $\text{CrO}_2\text{F}_2$  and  $\text{CrO}_2\text{Cl}_2$ , and very significantly so for  $\text{CrO}_2\text{H}_2$ . The O-M-O (or S-M-S) angle is below the tetrahedral value, except for  $\text{CrO}_2\text{H}_2$  and  $\text{CrO}_2(\text{CH}_3)_2$ . Optimized structures of two main group analogues,  $\text{SO}_2\text{F}_2$  and  $\text{SO}_2\text{H}_2$ , have also been included for comparison. They exhibit the large O-S-O and small Y-S-Y angles expected on the basis of the VSEPR model.<sup>[43]</sup>

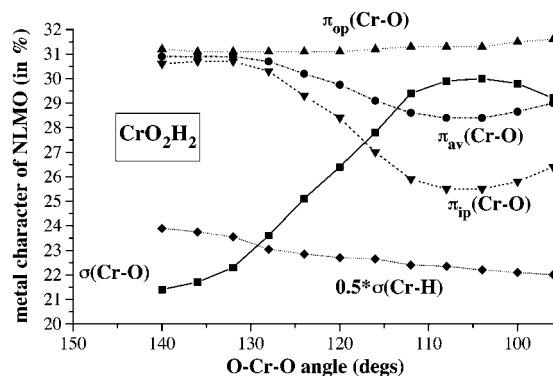
Figure 10 shows the NLMO analysis for chromyl fluoride. A designation of the oxo ligands as strong  $\pi$  donors (relative to their  $\sigma$ -donor ability) is not as appropriate as for  $\text{ZrO}_2$ , as the covalency of the  $\sigma(\text{Cr}-\text{O})$  NLMO is larger than that of either of the two  $\pi$  components (except for very large O-Cr-O angles). Nevertheless, both  $\sigma$  and  $\pi$  bonding to the oxo ligands

Figure 10. Dependence of the metal character (in%) of the bonding NLMOs in  $\text{CrO}_2\text{F}_2$  on O-M-O angle.

is significantly covalent. Deviations of the charge centroids for  $\sigma$ - and  $\pi_{\text{ip}}$ -bonding NBOs or NLMOs from the Cr-O axis are small (below  $5^\circ$  over the entire angle range of interest). The Cr-O  $\sigma$  covalency shows the expected increase with lower angles, with a maximum around  $105^\circ$ , close to the actual equilibrium bond angle ( $108.5^\circ$ ). Interestingly, the  $\pi_{\text{op}}$  covalency is considerably larger than the  $\pi_{\text{ip}}$  covalency (as for the free  $\text{MX}_2$  complexes; cf. Section III), and it *increases* with decreasing bond angle (in contrast to the  $\text{TiCl}_2\text{Y}_2$  complexes,

cf. Section IVA). It appears that the oxygen  $\pi$ -type lone pairs compete excellently for metal d orbitals with the weak fluoride ligand, and so the  $\pi_{\text{op}}(\text{Cr}-\text{O})$  bonding is very efficient even at small O-Cr-O angles. The  $\pi_{\text{ip}}$  curve shows the expected nonuniform behavior, with an overall larger covalency for the largest angles. However, as a result of the positive slope of the  $\pi_{\text{op}}$  curve, the  $\pi_{\text{av}}$  curve is very flat in the relevant angle range. Thus, the  $\pi$ -bonding covalency is large but overall relatively independent of the bond angle, due to partial cancellation between in-plane and out-of-plane components. We may thus conclude that the O-Cr-O angle probably is dominated by the Cr-O and Cr-F  $\sigma$  framework (however, the  $\pi$  bonding may influence the angle indirectly by forcing very short Cr-O bonds and thus a large metal d character in these bonds, cf. next section). The covalency of the  $\sigma(\text{Cr}-\text{F})$  NLMOs increases slightly with increasing O-Cr-O angle (the Cr-F  $\pi$  bonding is rather ionic and also shows little angular dependence, again due to cancellation between in-plane and out-of-plane components).

Let us now replace the weak ancillary  $\sigma$ - and  $\pi$ -donor fluoride ligand by the strong, exclusively  $\sigma$ -bonding hydride ligand to get  $\text{CrO}_2\text{H}_2$  (see Figure 11 for the NLMO analysis). Probably due to the competition with the very strong Cr-H  $\sigma$  bonding, the  $\sigma(\text{Cr}-\text{O})$  covalency is diminished compared to

Figure 11. Dependence of the metal character (in%) of the bonding NLMOs in  $\text{CrO}_2\text{H}_2$  on O-M-O angle.

$\text{CrO}_2\text{F}_2$ , particularly for large O-Cr-O angles. As an indirect consequence, the  $\pi_{\text{ip}}(\text{Cr}-\text{O})$  covalency appears to be considerably enhanced at large angles but decreases to similar values as in  $\text{CrO}_2\text{F}_2$  at lower angles. We also note significant bond bending of both  $\sigma$  and  $\pi_{\text{ip}}$  bonding NLMOs ( $10$ – $25^\circ$  over the relevant O-Cr-O angle range). Even at larger angles, the oxygen  $\pi_{\text{ip}}$  hybrids are rotated *towards* the second oxo ligand (the  $\sigma$ -bonding hybrids are rotated away), in contrast to the  $\text{TiCl}_2\text{Y}_2$  complexes (Section IVA). The  $\pi_{\text{op}}$  covalency varies relatively little; it increases slightly for low angles. The resulting  $\pi_{\text{av}}(\text{Cr}-\text{O})$  curve has a pronounced minimum around  $105^\circ$ , and the  $\pi$  covalency increases for larger angles. Likely as a consequence, the optimized O-Cr-O angle is  $112^\circ$  (see Table 3), that is larger than favored by  $\sigma(\text{Cr}-\text{O})$  bonding alone, and larger than for the chloride and fluoride (note also the large H-Cr-H angle). We suspect that the large angle dependence of both  $\sigma$  and  $\pi_{\text{ip}}$  covalency, as well as the



significant mixing between these two components, are connected to the presence of the strong ancillary hydride ligands.

Figure 12 examines the effect of replacing Cr in  $\text{CrO}_2\text{F}_2$  by its heavier homologue Mo. We note that the covalency of both  $\sigma$ - and  $\pi$ -type NLMOs is reduced, consistent with the expected larger ionicity of bonding in the 4d-metal complex. Otherwise, the situation is rather similar to that for the chromium complex. The slightly negative slope of the

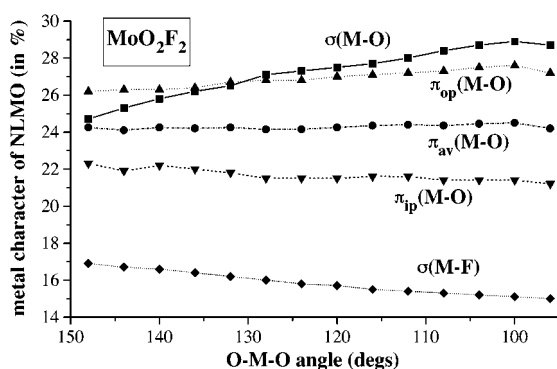


Figure 12. Dependence of the metal character (in %) of the bonding NLMOs in  $\text{MoO}_2\text{F}_2$  on O-M-O angle.

$\pi_{\text{ip}}(\text{Mo}-\text{O})$  curve is roughly compensated for by the positive slope of the  $\pi_{\text{op}}(\text{Cr}-\text{O})$  curve, leading to a very low overall angular dependence of the  $\pi$  bonding. We conclude that the observed angle seems to be dominated by the M–O  $\sigma$  bonding (bond bending of the NLMOs in  $\text{MoO}_2\text{F}_2$  is minor, as for  $\text{CrO}_2\text{F}_2$  above). The analysis for the thio-analogue  $\text{CrS}_2\text{F}_2$  (Figure S3 in Supporting Information) indicates very strong Cr–S  $\pi$  bonding, but also a relatively low overall angular dependence of the  $\pi_{\text{av}}$  curve (with a small positive slope in the relevant angle range).

Energy changes with X-M-X angle for a number of complexes are compared in Figure 13. The potential curves are all relatively flat for smaller angles than the equilibrium values. At larger angles, the X-M-X bending potentials increase steeply for the dioxo and dithio complexes. In contrast, the Cl-M-Cl potentials increase less pronouncedly. This holds in particular for  $\text{TiCl}_2(\text{CH}_3)_2$ , where the large-angle minimum is accompanied by an extremely flat potential curve. The comparison shows that there are large differences in the bending potentials for the various compounds studied.

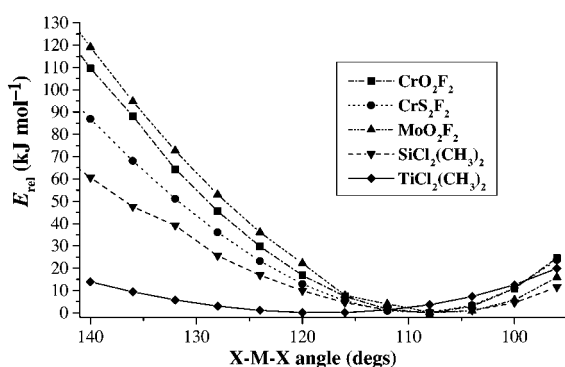


Figure 13. Comparison of energy profiles for the X-M-X angle coordinate in  $\text{MX}_2\text{Y}_2$  complexes. Relaxed scan.

We note also that the coupling between X-M-X and Y-M-Y angles is quite small. When changing the Cl-M-Cl angles in  $\text{SiCl}_2\text{Y}_2$  from  $96^\circ$  to  $140^\circ$ , the Y-M-Y angles increase merely by  $2.2^\circ$  (Y = H) or  $2.7^\circ$  (Y =  $\text{CH}_3$ ). For the transition metal complexes, the same increase in X-M-X angles *decreases* the Y-M-Y angles by about  $7-8^\circ$  (by  $11.3^\circ$  for  $\text{TiCl}_2\text{H}_2$ ). Changes in the Y-M-Y angles are found to be monotonous functions of those in the the X-M-X angles. The small interdependence of the angles suggests that the  $\text{MX}_2$  and  $\text{MY}_2$  fragments in such a  $\text{MX}_2\text{Y}_2$  complex do have to some extent an independent angle preference, of course modulated in addition by the other ligands. Thus, for example, O-Mo-O angles in  $\text{MoO}_2^{2+}$  fragments have angles in the  $101-105^\circ$  range for tetrahedral or octahedral complexes,<sup>[8, 10, 41, 42]</sup> as well as in the free fragment ion.<sup>[11]</sup> However, this is expected to change in the presence of strong ancillary  $\sigma$ -donor ligands like Y = H, alkyl (see above).

Typically, the M–X distances exhibit minima near the equilibrium bond angles (usually at somewhat lower angles). Changes in M–Y distances are small. The changes are monotonous when Y = H,  $\text{CH}_3$  (distances increase with increasing X-M-X angles for M = Si and decrease for transition metals) but tend to exhibit shallow minima for Y = F, Cl.

### C. Electronegativity and hybridization effects

The previous sections showed that  $\pi$  bonding may have an important effect on bond angles in  $d^0$  transition metal complexes. For  $\text{TiCl}_2(\text{CH}_3)_2$ , on which previous discussions of Bent's rule for  $d^0$  complexes have concentrated,<sup>[12, 13, 18]</sup> our analyses suggest that Ti–Cl  $\pi$  bonding acts to widen the Cl-Ti-Cl angle considerably. This molecule may thus not be a particularly good example to probe the influence of electronegativity differences within the  $\sigma$ -bonding framework only. It would be better to examine complexes in which  $\pi$  bonding is negligible. However, to find simple, covalently bound, heteroleptic  $\text{MX}_2\text{Y}_2$   $d^0$  model complexes, with sufficiently different ligand electronegativities but without  $\pi$  bonding, is not a trivial exercise (we assume in this case that X is the less electronegative ligand).

Table 4 summarizes the main optimized structural features of four systems studied,  $\text{TiH}_2(\text{CF}_3)_2$ ,  $\text{Ti}(\text{CH}_3)_2(\text{CF}_3)_2$ ,  $\text{Ti}(\text{SiH}_3)_2(\text{CH}_3)_2$ , and  $\text{Ti}(\text{SnH}_3)_2(\text{CH}_3)_2$ , together with the structural data for the corresponding main group analogues, where Ti is replaced by Si. In  $\text{Ti}(\text{CH}_3)_2(\text{CF}_3)_2$ , both X-M-X and Y-M-Y angles are slightly above the tetrahedral value, with the X-M-Y angle thus being small. This situation is not really covered by any simple model, although it is not

Table 4. Main DFT-optimized structural parameters for  $\sigma$ -bonded complexes.

$\text{MX}_2\text{Y}_2$	$d(\text{M}-\text{X})$ [Å]	$d(\text{M}-\text{Y})$ [Å]	$\angle(\text{X}-\text{M}-\text{X})$ [°]	$\angle(\text{X}-\text{M}-\text{Y})$ [°]	$\angle(\text{Y}-\text{M}-\text{Y})$ [°]
$\text{TiH}_2(\text{CF}_3)_2$	1.695	2.109	107.8	109.5	111.1
$\text{Ti}(\text{CH}_3)_2(\text{CF}_3)_2$	2.038	2.126	110.5	108.8	111.2
$\text{Ti}(\text{SiH}_3)_2(\text{CH}_3)_2$	2.636	2.037	106.4	109.3	113.2
$\text{Ti}(\text{SnH}_3)_2(\text{CH}_3)_2$	2.882	2.032	106.8	109.2	113.0
$\text{SiH}_2(\text{CF}_3)_2$	1.490	1.941	112.9	109.0	107.6
$\text{Si}(\text{CH}_3)_2(\text{CF}_3)_2$	1.883	1.941	116.3	108.6	105.6
$\text{Si}(\text{SiH}_3)_2(\text{CH}_3)_2$	2.368	1.920	108.1	109.5	110.7
$\text{Si}(\text{SnH}_3)_2(\text{CH}_3)_2$	2.622	1.924	108.5	109.6	109.9

as uncommon as one might think.<sup>[44]</sup> In  $\text{TiH}_2(\text{CF}_3)_2$ ,  $\text{Ti}(\text{SiH}_3)_2(\text{CH}_3)_2$ , and  $\text{Ti}(\text{SnH}_3)_2(\text{CH}_3)_2$ , the angles between the less electronegative substituents are smaller than  $109.5^\circ$ , whereas those between the more electronegative ones are larger. This is indeed just the opposite to the original expectations of Bent's rule. However, even the main group systems  $\text{Si}(\text{SiH}_3)_2(\text{CH}_3)_2$  and  $\text{Si}(\text{SnH}_3)_2(\text{CH}_3)_2$  violate Bent's rule by having large Y-Si-Y and small X-Si-X angles (Table 4).

Table 5 shows the results of NPA/NLMO hybridization analyses for these  $\sigma$ -bonded complexes. In general, the polarity of the NLMOs follows expectation, that is the M-X

Table 5. NPA/NLMO hybridization analyses for  $\sigma$ -bonded complexes and for  $\text{MCl}_2\text{Y}_2$  (M = Ti, Si; Y = H,  $\text{CH}_3$ ).<sup>[a]</sup>

	$\sigma(\text{M-X})$ NLMOs	$\sigma(\text{M-Y})$ NLMOs
$\text{TiH}_2(\text{CF}_3)_2$	$\sigma(\text{Ti-H})$ : 39.1 % Ti $\text{sd}^{2.90}$	$\sigma(\text{Ti-C})$ : 30.2 % Ti $\text{sd}^{4.34}$
$\text{Ti}(\text{CH}_3)_2(\text{CF}_3)_2$	$\sigma(\text{Ti-CH}_3)$ : 30.3 % Ti $\text{sd}^{4.78}$	$\sigma(\text{Ti-CF}_3)$ : 29.0 % Ti $\text{sd}^{4.10}$
$\text{Ti}(\text{SiH}_3)_2(\text{CH}_3)_2$	$\sigma(\text{Ti-Si})$ : 36.4 % Ti $\text{sd}^{2.58}$	$\sigma(\text{Ti-C})$ : 27.6 % Ti $\text{sd}^{5.74}$
$\text{Ti}(\text{SnH}_3)_2(\text{CH}_3)_2$	$\sigma(\text{Ti-Sn})$ : 38.0 % Ti $\text{sd}^{2.42}$	$\sigma(\text{Ti-C})$ : 27.3 % Ti $\text{sd}^{6.18}$
$\text{SiH}_2(\text{CF}_3)_2$	$\sigma(\text{Si-H})$ : 41.9 % Si $\text{sp}^{1.74}$	$\sigma(\text{Si-C})$ : 31.2 % Si $\text{sp}^{2.06}$
$\text{Si}(\text{CH}_3)_2(\text{CF}_3)_2$	$\sigma(\text{Si-CH}_3)$ : 28.6 % Si $\text{sp}^{1.54}$	$\sigma(\text{Si-CF}_3)$ : 28.9 % Si $\text{sp}^{1.98}$
$\text{Si}(\text{SiH}_3)_2(\text{CH}_3)_2$	$\sigma(\text{Si-Si})$ : 47.2 % Si $\text{sp}^{1.99}$	$\sigma(\text{Si-C})$ : 29.1 % Si $\text{sp}^{1.82}$
$\text{Si}(\text{SnH}_3)_2(\text{CH}_3)_2$	$\sigma(\text{Si-Sn})$ : 50.6 % Si $\text{sp}^{2.05}$	$\sigma(\text{Si-C})$ : 29.2 % Si $\text{sp}^{1.66}$
$\text{TiCl}_2(\text{CH}_3)_2$	$\sigma(\text{Ti-C})$ : 32.6 % Ti $\text{sd}^{5.47}$	$\sigma(\text{Ti-Cl})$ : 17.4 % Ti $\text{sd}^{3.09}$
$\text{TiCl}_2\text{H}_2$	$\sigma(\text{Ti-H})$ : 42.2 % Ti $\text{sd}^{3.56}$	$\sigma(\text{Ti-Cl})$ : 17.6 % Ti $\text{sd}^{3.35}$
at $E_{\text{Lewis}}$ structure <sup>[b]</sup>	$\sigma(\text{Ti-H})$ : 40.8 % Ti $\text{sd}^{3.38}$	$\sigma(\text{Ti-Cl})$ : 17.5 % Ti $\text{sd}^{2.84}$
$\text{SiCl}_2(\text{CH}_3)_2$	$\sigma(\text{Si-C})$ : 28.1 % Si $\text{sp}^{1.08}$	$\sigma(\text{Si-Cl})$ : 23.4 % Si $\text{sp}^{1.86}$
$\text{SiCl}_2\text{H}_2$	$\sigma(\text{Si-H})$ : 42.0 % Si $\text{sp}^{1.33}$	$\sigma(\text{Si-Cl})$ : 25.3 % Si $\text{sp}^{1.93}$
at $E_{\text{Lewis}}$ structure <sup>[b]</sup>	$\sigma(\text{Si-H})$ : 42.6 % Si $\text{sp}^{1.12}$	$\sigma(\text{Si-Cl})$ : 25.0 % Si $\text{sp}^{2.09}$

[a] Results at the optimized equilibrium structures unless noted otherwise. The metal natural atomic orbital (NAO) contributions to the corresponding NLMOs and their composition are given. p-NAO contributions are small for M = Ti (<2%), and d-NAO contributions are small for M = Si ( $\leq 1\%$ ). [b] At the structures optimized relative to the energy of a singly bonded NBO Lewis structure. These conform to Bent's rule for both  $\text{TiCl}_2\text{H}_2$  and  $\text{SiCl}_2\text{H}_2$  (cf. Table 2).

bonds are indeed more covalent than the M-Y bonds. However, the difference in polarity between  $\text{CH}_3$  and  $\text{CF}_3$  ligands turns out to be marginal, so that the  $\text{M}(\text{CH}_3)_2(\text{CF}_3)_2$  complexes are not very good examples. In  $\text{TiH}_2(\text{CF}_3)_2$ ,  $\text{Ti}(\text{SiH}_3)_2(\text{CH}_3)_2$ , and  $\text{Ti}(\text{SnH}_3)_2(\text{CH}_3)_2$ , more s character is connected to the smaller angles (between the less electronegative substituents) and less s character to the larger angles (between the more electronegative substituents). This distribution of the s character is as predicted by Landis et al., based on  $\text{sd}^x$  hybrid orbital strength functions,<sup>[18]</sup> but contrasts with the suggestion of Jonas et al.<sup>[14]</sup> that more d character should be connected to the larger angle. The analysis of Jonas et al. was based on the NBO compositions computed for  $\text{TiCl}_2(\text{CH}_3)_2$ . The entry for this complex in Table 5 indicates that the large d character for the Ti-C bonds observed by Jonas et al. is found also for the NLMOs, which we take to be a more reliable measure than the NBO hybridizations (see Computational Methods). Similarly,  $\text{TiCl}_2\text{H}_2$  exhibits the larger metal d character in the Ti-Cl bonds. There is thus a clear discrepancy between the hybrid distributions for the exclusively  $\sigma$ -bonded examples and those for  $\text{TiCl}_2\text{Y}_2$  (Y = H,  $\text{CH}_3$ ) complexes, which involve Ti-Cl  $\pi$  bonding.

At the  $E_{\text{Lewis}}$  structures of  $\text{MCl}_2\text{H}_2$  (M = Si, Ti), which both obey Bent's rule (Table 2), the differences in the central-atom

hybridizations are even more pronounced. With M = Ti, lower d character is still seen for the M-Cl bonds. However, this means now that the larger d character pertains to the larger H-M-H angles (see Table 5). We have thus arrived again at a situation consistent with Landis' hybrid orbital strength functions,<sup>[18]</sup> but with the smaller angle between the more electronegative ligands. The inverted situation at the  $E_{\text{opt}}$  structures of the two  $\text{TiCl}_2\text{Y}_2$  complexes may thus be related to the presence of Ti-Cl  $\pi$  bonding and coincides with the presence of a significant deviation of the Ti-Cl  $\sigma$  bonding NBO from the Ti-Cl axis at the optimized structure ( $23.7^\circ$  on the chlorine hybrid side, ca.  $5^\circ$  for the metal hybrid). As the rotation of the  $\sigma$ -bonding hybrids at the equilibrium structure is towards the second chloride ligand, the effective angle between the Ti-Cl  $\sigma$ -bonding charge centroids is smaller than the optimized Cl-Ti-Cl angle. The bond bending reduces thereby the effective angle between the Ti-Cl bonds, and the hybrid composition is not expected to reflect the actual bond angles. It is thus clear that a rationalization of bond angles with hybridization arguments is difficult in these systems. Interestingly, the bond bending is very small ( $1.7^\circ$  for the chlorine hybrid) at the  $E_{\text{Lewis}}$  structure of  $\text{TiCl}_2\text{H}_2$ .

For  $\text{SiX}_2(\text{CH}_3)_2$  (X =  $\text{SiH}_3$ ,  $\text{SnH}_3$ ), the unexpectedly small X-Si-X angles are accompanied by a larger p-character in the Si-X bonds than in the Si-C bonds, in spite of the less polar bonding. This does clearly violate Bent's rule in its original formulation. Possibly, the rather diffuse bonding orbitals employed by the  $\text{SiH}_3$  and  $\text{SnH}_3$  substituents make it more favorable for the central atom to direct considerable p-character towards these groups. It appears thus that the relative substituent orbital size (i.e. overlap considerations) overrides electronegativity differences in these cases. This is consistent with an extension of Bent's rule due to Huheey et al., which assigns the larger hybrid s character to the stronger covalent interactions and thus incorporates both electronegativity and overlap aspects.<sup>[45]</sup> We have also found inverted carbon hybridization for mercurimethanes [ $\text{CH}_n(\text{HgX})_{4-n}$ ], where hydrogen 1s orbitals compete with mercury 6s orbitals for the carbon bonding hybrids.<sup>[46]</sup> Of the four ligand combinations studied in this section, only the combination X = H, Y =  $\text{CF}_3$  thus appears to fulfill the expectations, that is behavior according to Bent's original rule is observed with  $\text{SiH}_2(\text{CF}_3)_2$  but an "inverted" structure is found for  $\text{TiH}_2(\text{CF}_3)_2$ . This shows that it is difficult to select suitable reference compounds to discuss the electronegativity effects on hybridization and bond angles alone. We conclude that no simple relations between ligand electronegativity, hybridization, and bond angles are apparent for these  $\text{d}^0$  complexes, even in the absence of  $\pi$  bonding.

Hybridization analyses for the dichalcogenido complexes are given in Table S1 in the Supporting Information. We note here only that the metal d character of the  $\sigma(\text{M-O})$  NLMOs in the dioxo complexes is very large, generally much larger than the d character directed towards the ancillary ligands. This holds regardless of the electronegativity of the ancillary ligands and is likely due to the very short multiple bonds, which force their  $\sigma$  components to utilize significant metal d character. In contrast, in  $\text{CrS}_2\text{F}_2$  more metal d character pertains to the  $\sigma(\text{Cr-F})$  than to the  $\sigma(\text{Cr-S})$  NLMOs.

As a general comment, we note that the NLMO/NPA hybridizations shown in Table 5 (cf. also Table S1 in Supporting Information) indicate considerable “hybridization defects”<sup>[17, 47]</sup> in all cases. Thus, for the silicon compounds the average *s* character is considerably larger than that implied by the orthogonal  $sp^3$  hybrids one usually associates with tetrahedral coordination. In contrast, the average metal *s* character for the  $\sigma$ -bonding NLMOs in the transition metal complexes is smaller than implied by  $sd^3$  hybridization.<sup>[48]</sup> As has been discussed in detail for the heavier *p*-block main group case,<sup>[17, 47]</sup> ideal orthogonal  $sp^n$  hybrids would require *s*- and *p*-valence orbitals of similar radial extent. However, the valence *s* orbitals are much more contracted than the *p* orbitals, and thus the *s* character is generally larger than expected within the traditional counting rules used to relate bond angles to hybridization. Similarly, the 3*d* orbitals of titanium in the present  $d^0$  complexes have obviously a smaller radial extent than the 4*s* orbitals with which they have to be hybridized. Therefore, the average *d* character is larger than what would be obtained with orthogonal  $sd^3$  hybrids. In simple homoleptic hydride complexes, hybridization defects tend to be moderate,<sup>[18]</sup> but in the presence of more electronegative ligands they obviously become sizeable.

## V. Conclusion

The bonding analyses presented in this work are based mostly on the NBO/NLMO procedure of Weinhold et al.<sup>[26, 27]</sup> The data do thus of course contain some degree of arbitrariness, as is true for any type of population analysis or density-matrix partitioning scheme. Complications arise also from the inherently ill-defined nature of in-plane  $\pi$  and  $\sigma$  bonding for nonlinear molecules. However, we have been careful to discuss only trends, mostly for variations in the structure of a given complex. We expect that the following general conclusions drawn will remain unaltered when using alternative interpretational schemes:

- Ligand-to-metal  $\pi$  bonding tends to be much more important in early transition metal  $d^0$  complexes than for analogous main group species, due to the ready availability of *inner* metal *d* orbitals. The influence of  $\pi$  bonding on bond angles may thus also be significant.
- Due to the variety of possible orientations of the different metal *d* orbitals available as acceptors for  $\pi$  bonding, the actual angular dependence of  $\pi$  bonding may be complicated. This holds in particular for the in-plane  $\pi$  bonding in  $MX_2$  molecules or fragments.
- In  $d^0$   $MX_2$  complexes,  $\pi$  bonding may be stronger either in linear or in bent structures.  $\pi$  bonding appears to favor the bent structure for the “strong  $\pi$ -donor case”  $ZrO_2$ , but the linear structure for the “weak  $\pi$ -donor case”  $ScF_2^+$ . However, near the bent equilibrium structures,  $\pi$  bonding seems to favor smaller angles in both complexes.
- The “inverse Bent’s rule” structure of  $TiCl_2Y_2$  ( $Y = H, CH_3$ ) is at least in part due to significant Ti–Cl  $\pi$  bonding, acting to increase the Cl–Ti–Cl angle and to decrease the Y–Ti–Y angle.  $\pi$  Bonding also counteracts the normal

electronegativity-driven “Bent’s rule” distortions for main group species like  $SiCl_2Y_2$ ,<sup>[39]</sup> but there its influence is not sufficient to reverse the relative order of the angles.

- For  $MX_2Y_2$  complexes with strong  $\pi$ -donor ligands *X* but weak ancillary ligands *Y*, like  $CrO_2F_2$  or  $MoO_2F_2$ , out-of-plane M–X  $\pi$  bonding is larger than in-plane  $\pi$  bonding and it favors smaller X–M–X angles. As a result of the partial compensation between the angular dependence of the different  $\pi$  bonding contributions, the overall influence of  $\pi$  bonding on bond angle may be small. However, when the ancillary ligand *Y* is a strong  $\sigma$  donor, as in  $CrO_2H_2$ , the in-plane  $\pi$ -bonding component starts again to dominate the angular dependence, and  $\pi$  bonding apparently favors a larger O–M–O angle.

It is difficult to isolate the influence of ligand electronegativity on the bond angles from the  $\pi$  bonding effects, due to the need to find suitable  $\sigma$ -bonded model systems. Of the four complexes studied here, only  $MH_2(CF_3)_2$  turned out to cleanly obey Bent’s rule for the main group case ( $M = Si$ ), whereas the others exhibit more irregular behavior. For  $TiH_2(CF_3)_2$ , an “inverse Bent’s rule structure” was found. The hybridization analyses indicate less *d* character in the bonds to the less electronegative ligands, in contrast to our analyses and previous ones<sup>[14]</sup> for  $TiCl_2Y_2$  ( $Y = H, CH_3$ ). For the latter compounds, the relation between hybridization and bond angles is obscured by the occurrence of significant “bond bending” of the relevant  $\sigma$ -bonding localized MOs. This is in turn related to the presence of in-plane  $\pi$  bonding. For  $SiX_2(CH_3)_2$  complexes with  $X = SiH_3, SnH_3$ , Bent’s rule in its original version is violated even in the main group case, most likely due to disparate substituent orbital sizes (i.e. overlap considerations override electronegativity effects<sup>[45]</sup>).

Overall, the interdependence of  $\pi$  bonding, substituent electronegativity, and  $\sigma$ -bonding influences on bond angles in  $d^0$  complexes appears to be considerably more complicated than for their main group analogues. This should not surprise us, given the larger number and more variable directionality of valence orbitals available for transition metal systems. As a result, simple models like Bent’s rule are not as useful as for *p*-block main group compounds. More refined interpretations have to be given, and the present work is a step into that direction.

While the present model study has focussed only on the simplest triatomic  $MX_2$  complexes and on pseudotetrahedral  $MX_2Y_2$  systems, it is clear that very similar considerations will hold also for other ligand combinations and for other coordination numbers. For example, density functional and *ab initio* calculations on heteroleptic complexes bearing both  $\pi$ -donor and exclusive  $\sigma$ -donor ligands have been carried out also for five-<sup>[49, 50]</sup> and six-coordinate<sup>[51]</sup> complexes. In all of these cases, a very pronounced competition between  $\pi$ - and  $\sigma$ -bonding contributions has been found, leading in many cases to rather striking structural features.<sup>[49–51]</sup> In addition to the structural aspects, on which we have concentrated in the present study, it is obvious that reactivity is similarly dependent on  $\pi$  bonding and ligand electronegativity. This holds, for example, for the stereochemical outcome of chemical reactions. As many  $d^0$  complexes are of significant importance, for

example in catalysis and metalloenzymes, there remains a considerable need to develop such structure–bonding relationships.

### Acknowledgment

This work was supported by Deutsche Forschungsgemeinschaft (DFG) through a ‘Heisenbergstipendium’ (since 1998), and by Fonds der Chemischen Industrie. I am grateful to Drs. Clark R. Landis (U. Wisconsin), Gernot Frenking (Marburg), Arne Haaland (Oslo), and Michael Bühl (Zürich) for stimulating discussions, and for helpful comments on the manuscript.

- [1] See, for example: a) M. Kaupp, P. von R. Schleyer, H. Stoll, H. Preuss, *J. Chem. Phys.* **1991**, *94*, 1360; b) L. Seijo, Z. Barandiaran, S. Huzinaga, *J. Chem. Phys.* **1991**, *94*, 762; c) M. Kaupp, P. von R. Schleyer, H. Stoll, H. Preuss, *J. Am. Chem. Soc.* **1991**, *113*, 6012, and references therein. See ref. [1c] for arguments that justify the classification of these systems as transition metal complexes.
- [2] P. M. Morse, G. S. Girolami, *J. Am. Chem. Soc.* **1989**, *111*, 4114; A. Haaland, A. Hammel, K. Rypdal, H. V. Volden, *J. Am. Chem. Soc.* **1990**, *112*, 4547; V. Pfennig, K. Seppelt, *Science* **1996**, *271*, 626; S. Kleinhenz, V. Pfennig, K. Seppelt, *Chem. Eur. J.* **1998**, *4*, 1687; S. Kleinhenz, M. Schubert, K. Seppelt, *Chem. Ber.* **1997**, *130*, 903.
- [3] S. K. Kang, H. Tang, T. A. Albright, *J. Am. Chem. Soc.* **1993**, *115*, 1971.
- [4] C. R. Landis, T. Cleveland, T. K. Firman, *J. Am. Chem. Soc.* **1995**, *117*, 1859; M. Kaupp, *J. Am. Chem. Soc.* **1996**, *118*, 3018; M. Kaupp, *Chem. Eur. J.* **1998**, *4*, 1678.
- [5] M. Kaupp, unpublished results.
- [6] It has been suggested that core polarization is the sole factor that gives rise to the non-VSEPR structures of  $d^0$  systems (see, for example: I. Bytheway, R. J. Gillespie, T.-H. Tang, R. W. F. Bader, *Inorg. Chem.* **1995**, *34*, 2407; I. Bytheway, P. L. A. Popelier, R. J. Gillespie, *Can. J. Chem.* **1996**, *74*, 1059). However, even for very ionic alkaline earth  $MX_2$  compounds it has been demonstrated earlier that core polarization alone is not sufficient to explain the distortions, and that the d-orbital participation in covalent bonding has to be considered.<sup>[1]</sup> Obviously, the importance of core polarization is even less pronounced for more covalent complexes of the transition metals.<sup>[18]</sup> Moreover, deformations in the Laplacian of the charge density were even found when, for  $TiCl_2(CH_3)_2$ , a valence density was added to a frozen atomic core (R. W. F. Bader, R. J. Gillespie, F. Martin, *Chem. Phys. Lett.* **1998**, *290*, 488). This makes it impossible to identify any relation of these features in the  $\Delta\rho$  distribution to the core-polarization model.
- [7] a) A. Demolliens, Y. Jean, O. Eisenstein, *Organometallics* **1986**, *5*, 1457; b) S. K. Kang, T. A. Albright, O. Eisenstein, *Inorg. Chem.* **1989**, *28*, 1611; c) C. A. Jolly, D. S. Marynick, *Inorg. Chem.* **1989**, *28*, 2893; d) M. Kaupp, P. von R. Schleyer, *J. Am. Chem. Soc.* **1992**, *114*, 491.
- [8] See, for example: a) W. P. Griffith, T. D. Wickins, *J. Chem. Soc. A* **1968**, 400; b) K. Tatsumi, R. Hoffmann, *Inorg. Chem.* **1980**, *19*, 2656; c) D. M. P. Mingos, *J. Organomet. Chem.* **1979**, *179*, C29; d) D. C. Brower, J. L. Templeton, D. M. P. Mingos, *J. Am. Chem. Soc.* **1987**, *109*, 5203.
- [9] See, for example: F. A. Cotton, G. Wilkinson, *Advanced Inorganic Chemistry*, 5th ed., Wiley, New York, **1988**.
- [10] See, for example: W. A. Nugent, J. M. Mayer, *Metal-Ligand Multiple Bonds*, Wiley, New York, **1988**, and references therein.
- [11] P. Pykkö, T. Tamm, *J. Phys. Chem. A* **1997**, *101*, 8107.
- [12] G. S. McGrady, A. J. Downs, D. C. McKean, A. Haaland, W. Scherer, H.-P. Verne, H. V. Volden, *Inorg. Chem.* **1996**, *35*, 4713.
- [13] a) V. Jonas, G. Frenking, M. T. Reetz, *J. Comput. Chem.* **1992**, *13*, 919; b) S. Berger, W. Bock, G. Frenking, V. Jonas, F. Müller, *J. Am. Chem. Soc.* **1995**, *117*, 3820.
- [14] V. Jonas, C. Böhme, G. Frenking, *Inorg. Chem.* **1996**, *35*, 2097.
- [15] A. V. Belyakov, V. S. Zavgorodnii, V. S. Mastryukov, *J. Struct. Chem.* **1989**, *30*, 27; *Zh. Strukt. Khim.* **1989**, *30*, 34.
- [16] H. A. Bent, *Chem. Rev.* **1961**, *61*, 275.
- [17] W. Kutzelnigg, *Angew. Chem.* **1984**, *96*, 262; *Angew. Chem. Int. Ed. Engl.* **1984**, *23*, 272.
- [18] C. R. Landis, T. K. Firman, D. M. Root, T. Cleveland, *J. Am. Chem. Soc.* **1998**, *120*, 1842.
- [19] C. R. Landis, personal communication.
- [20] A. D. Becke, *Phys. Rev. A* **1988**, *38*, 3098; J. P. Perdew, *Phys. Rev. B* **1986**, *33*, 8822.
- [21] Gaussian 94, Revisions B2, G2, M. J. Frisch, G. W. Trucks, H. B. Schlegel, P. M. W. Gill, B. G. Johnson, M. A. Robb, J. R. Cheeseman, T. Keith, G. A. Petersson, J. A. Montgomery, K. Raghavachari, M. A. Al-Laham, V. G. Zakrzewski, J. V. Ortiz, J. B. Foresman, C. Y. Peng, P. Y. Ayala, W. Chen, M. W. Wong, J. L. Andres, E. S. Replogle, R. Gomperts, R. L. Martin, D. J. Fox, J. S. Binkley, D. J. Defrees, J. Baker, J. P. Stewart, M. Head-Gordon, C. Gonzalez, and J. A. Pople, Gaussian, Inc., Pittsburgh, **1995**.
- [22] a) M. Dolg, U. Wedig, H. Stoll, H. Preuss, *J. Chem. Phys.* **1987**, *86*, 866; D. Andrae, U. Häußermann, M. Dolg, H. Stoll, H. Preuss, *Theor. Chim. Acta* **1990**, *77*, 123.
- [23] A. Bergner, M. Dolg, W. Küchle, H. Stoll, H. Preuss, *Mol. Phys.* **1993**, *80*, 1431.
- [24] d-Type polarization functions have been taken from: *Gaussian Basis Sets for Molecular Calculations* (Ed.: S. Huzinaga) Elsevier, New York, **1984**.
- [25] T. H. Dunning, H. Hay in *Methods of Electronic Structure Theory; Modern Theoretical Chemistry, Vol. 3*, (Ed. H. F. Schaefer III), Plenum, New York, **1977**.
- [26] See, for example: a) A. E. Reed, F. Weinhold, *J. Chem. Phys.* **1985**, *83*, 1736; b) A. E. Reed, L. A. Curtiss, F. Weinhold, *Chem. Rev.* **1988**, *88*, 899, and references therein.
- [27] L. A. Curtiss, D. J. Pochatko, A. E. Reed, F. Weinhold, *J. Chem. Phys.* **1985**, *82*, 2679.
- [28] For a discussion see, for example: E. J. Baerends, O. Gritsenko, *J. Phys. Chem. A* **1997**, *101*, 5383.
- [29] An entirely different view has been put forward, which is however not backed by any quantum chemical analyses: M. Gerloch, E. C. Constable, *Transition Metal Chemistry: The Valence Shell in d-Block Chemistry*, VCH, Weinheim, **1994**.
- [30] For early discussions, see also: E. F. Hayes, *J. Phys. Chem.* **1966**, *70*, 3740; C. A. Coulson, *Nature* **1969**, *221*, 1106.
- [31] a) P. E. M. Siegbahn, *J. Phys. Chem.* **1993**, *97*, 9096; b) G. V. Chertihin, L. Andrews, *J. Phys. Chem.* **1995**, *99*, 6356.
- [32] M. Kaupp, O. P. Charkin, P. von R. Schleyer, *Organometallics* **1992**, *11*, 2767.
- [33] NPA metal charges at the respective equilibrium structures are 2.028, 1.732, and 1.416 for  $ScF_2^+$ ,  $ZrO_2$ , and  $TiO_2$ , respectively. Another reason for choosing  $ZrO_2$  over  $TiO_2$  is the better behavior of the NBO Lewis structures over the entire angle range covered.
- [34] The  $NH_2$  groups favor an in-plane conformation to maintain  $\pi_{op}$  bonding. Rotation out of the plane is coupled to an increase in the N-Ba-N bending angle. See ref. [7d].
- [35] A. J. Bridgeman, *J. Chem. Soc. Dalton Trans.* **1997**, 2887.
- [36] We have repeated the DFT calculations of ref. [35] with much larger basis sets. Our results confirm the very shallow bending potentials of ref. [37].
- [37] M. Kaupp, P. von R. Schleyer, H. Stoll, M. Dolg, *J. Am. Chem. Soc.* **1992**, *114*, 8202.
- [38] M. Kaupp, O. P. Charkin, P. von R. Schleyer, *Organometallics* **1992**, *11*, 2765–2767.
- [39] See, for example: A. E. Reed, P. von R. Schleyer, *J. Am. Chem. Soc.* **1987**, *109*, 7362; A. E. Reed, P. von R. Schleyer, *Inorg. Chem.* **1988**, *27*, 3969. Electronegativity-driven distortions are largest for heavier p-block elements, where negative hyperconjugation is less pronounced: M. Kaupp, P. von R. Schleyer, *J. Am. Chem. Soc.* **1993**, *115*, 1061.
- [40] Note also, that the inclusion of the non-Lewis bonding contributions does in both cases shorten the M–Cl bonds considerably (more so for  $M=Ti$ ). However, while the Si–H bond in  $SiCl_2H_2$  is lengthened slightly in turn (it acts as an acceptor for negative hyperconjugation), the Ti–H bond in  $TiCl_2H_2$  also contracts. This is consistent with a  $\pi$ -bonding mechanism related to negative hyperconjugation for the main group system but not for the  $d^0$  complex.

- [41] See, for example: R. J. French, L. Hedberg, K. Hedberg, G. L. Lard, B. M. Johnson, *Inorg. Chem.* **1983**, *22*, 892; C. J. Marsden, L. Hedberg, K. Hedberg, *Inorg. Chem.* **1982**, *21*, 1115. *Tables of Interatomic Distances and Configurations in Molecules and Ions* (Ed. L. E. Sutton), The Chemical Society, London **1958**; D. R. Lide Jr., D. E. Mann, R. M. Fristrom, *J. Chem. Phys.* **1957**, *26*, 734.
- [42] See, for example: R. J. Deeth, *J. Phys. Chem.* **1993**, *97*, 11625; S. Dasgupta, T. Yamasaki, W. A. Goddard, *J. Chem. Phys.* **1996**, *104*, 2898; T. V. Russo, R. L. Martin, P. J. Hay, A. K. Rappé, *J. Chem. Phys.* **1995**, *102*, 9315; J. Cioslowski, P. R. Surján, *THEOCHEM* **1992**, *87*, 9.
- [43] See, for example: R. J. Gillespie, I. Hargittai, *The VSEPR Model of Molecular Geometry*, Allyn and Bacon, Boston **1991**; R. J. Gillespie, E. A. Robinson, *Angew. Chem.* **1996**, *108*, 539; *Angew. Chem. Int. Ed. Engl.* **1996**, *35*, 495
- [44] For further computational examples see, for example: M. H. Palmer, *J. Mol. Struct.* **1997**, *405*, 179, 193.
- [45] J. E. Huuhey, E. Keiter, R. Keiter, *Inorganic Chemistry*, 4th ed., Harper Collins College Publishers, New York, **1993**; S. O. Grim, H. J. Plastas, C. L. Huuhey, J. E. Huuhey, *Phosphorus Relat. Group V Elem.* **1971**, *1*, 61; J. E. Huuhey *Inorg. Chem.* **1981**, *20*, 4035.
- [46] M. Kaupp, O. L. Malkina, *J. Chem. Phys.* **1998**, *108*, 3648.
- [47] W. Kutzelnigg, *THEOCHEM* **1988**, *169*, 403.
- [48] As the  $\pi$  bonding is largely associated with metal d orbitals, the net metal populations obtained from the natural population analyses exhibit even larger d character.
- [49] T. R. Ward, H.-B. Bürgi, F. Gillardoni, J. Weber, *J. Am. Chem. Soc.* **1997**, *119*, 11974.
- [50] M. Kaupp, *Chem. Eur. J.* **1998**, *4*, 2059.
- [51] a) M. Kaupp, *Angew. Chem.* **1999**, *111*, 3219; *Angew. Chem. Int. Ed.* **1999**, *38*, 3034; b) for other distortions of  $d^0$  octahedral structures see, for example: J. R. Clark, A. L. Pulvirenti, P. E. Fanwick, M. Sigalas, O. Eisenstein, I. P. Rothwell, *Inorg. Chem.* **1997**, *36*, 3623; C. A. Bayse, M. B. Hall, *Organometallics* **1998**, *17*, 4861.

Received: April 9, 1999 [F 1720]